Geosynthetics for natural disaster prevention and mitigation -Japanese challenge-

Jiro Kuwano
Saitama University, Japan

Yoshiyuki Mohri
Ibaraki University, Japan

Yoshiaki Kikuchi & Yasuo Nihei
Tokyo University of Science, Japan

Junichi Koseki & Kenji Watanabe
University of Tokyo, Japan

ABSTRACT: Japan is a country of a variety of serious natural hazards. It is composed of many islands and has long coastlines. The islands are mostly mountainous with volcanos. As Japan is located on the four earth's crusts, there are numerous active faults which cause unstable natural slopes and, of course, strong earth-quakes. Japan has been repeatedly hit by earthquakes, some of which induced tsunamis. Japan often suffers heavy rains caused by weather fronts, typhoons and their combinations. Due probably to the global warming, the number of sudden downpours is increasing. Japan is affected by about 10 typhoons annually, which cause not only heavy rains but also high waves causing damage of coastlines. Application of geosynthetic technology has increased in Japan because of its high strength and durability. This report intro-duces Japanese challenges to utilize geosynthetic technologies to mitigate natural disasters. It covers reinforced embankments resisting overtopping caused by tsunami and river flood, geotubes for coastal protection especially for Japanese severe environment such as high waves, reinforced soil wall and/or geonet for rock fall protection works, and recent challenges to natural hazards.

Keywords: geosynthetics, natural disaster, mitigation

1 INTRODUCTION

Japan is a country of a variety of serious natural hazards. It is composed of many islands and has long coastlines. The islands are mostly mountainous with volcanos. As Japan is located on the four earth's crusts, there are numerous active faults which cause unstable natural slopes and, of course, strong earthquakes. Japan has been repeatedly hit by earthquakes, some of which induced tsunamis. The 2011 off the Pacific coast of Tohoku Earthquake (The 2011 Tohoku Earthquake) of M_w=9.0 with a huge source region of about 450 km by 200 km occurred on March 11, 2011. It is the largest earthquake ever recorded in Japan and the fourth largest in the world after 1900 (USGS, 2012). Wide area in the Tohoku and Kanto regions were strongly shaken by the earthquake. At some locations, very high accelerations of more than 1000 gal, or even more than 2000 gal at particular sites, were recorded. Large settlement, sliding failure, and collapsing of conventional type retaining wall of unreinforced soil structure, such as road and railway embankments, earth dams and housing sites, occurred by the earthquake. Almost 20,000 people are dead or missing by the 2011 Tohoku earthquake. Tsunami was the most serious impact of the earthquake. Inundation height and run-up height were as high as about 40 m (Tsunami Joint Survey Group, 2012). It killed thousands of lives and caused extensive damage of various structures such as seawalls and bridges. Many seawalls and river dikes were washed out by the tsunami. However, many reinforced soil walls survived the tsunami impact, though they were partly or fully submerged. With respect to the performances of reinforced soil walls, various teams went to the wall sites and the damage was reported in Kuwano et al. (2012, 2014) as shown in Figure 1 and Table 1. The damage of reinforced soil walls, i.e. steel strip walls (Terre Armee), multi-anchor walls and geogrid walls, was classified into four levels, namely, ultimate limit state, restorability limit state, serviceability limit state. The ultimate limit state is only less than 1% of investigated walls for all the three types. More than 90% of the walls show no damage. It is to be mentioned that the 2011 Tohoku earthquake was so huge, and its aftershocks were also very strong. Such

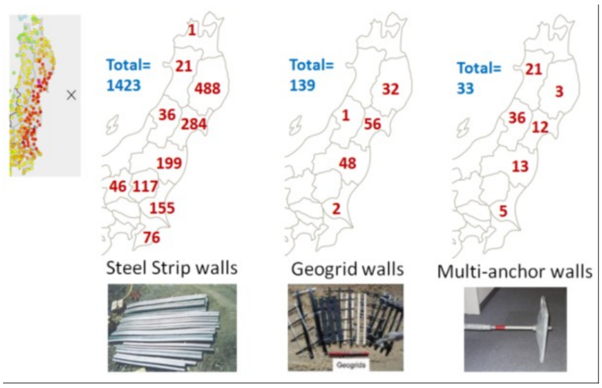

Figure 1. Site investigation of earthquake damage to reinforced soil wall in the 2011 Tohoku earthquake (Miyata, 2012, Kuwano et al., 2014).

Table 1. Damage statistics of reinforced soil wall in the 2011 Tohoku earthquake (Miyata, 2012)

	Steel strip walls	Geogrid walls	Multi-anchor walls
Ultimate limit state	0.3%	0.7%	0%
Restorability limit state	1.0%	4.3%	0%
Serviceability limit state	7.0%	0.7%	3.0%
No damage	91.7%	94.3%	97.0%

a strong seismic load was not considered in the design of reinforced soil walls. However, most of the walls showed very high seismic resistance in the earthquake. As the main concern of this report is “geosynthetics for natural disaster prevention and mitigation”, stability of reinforced soil walls with respect to seismic motion is not discussed in this report. However, stability of reinforced soil walls against hydraulic impact is reported.

Japan often suffers heavy rains caused by weather fronts, typhoons and their combinations. Due probably to the global warming, the number of sudden downpours is increasing as shown in Figure 2. Japan is affected by about 10 typhoons annually, which cause not only heavy rains but also high waves causing damage of coastlines. Application of geosynthetic technology has increased in Japan because of its high strength and durability. This report introduces Japanese challenges to utilize geosynthetic technologies to mitigate natural disasters. It covers reinforced embankments resisting overtopping caused by tsunami and river flood, geotubes for coastal protection especially for Japanese severe environment such as high waves, reinforced soil wall and/or geonet for rock fall protection works, and recent challenges to natural hazards.

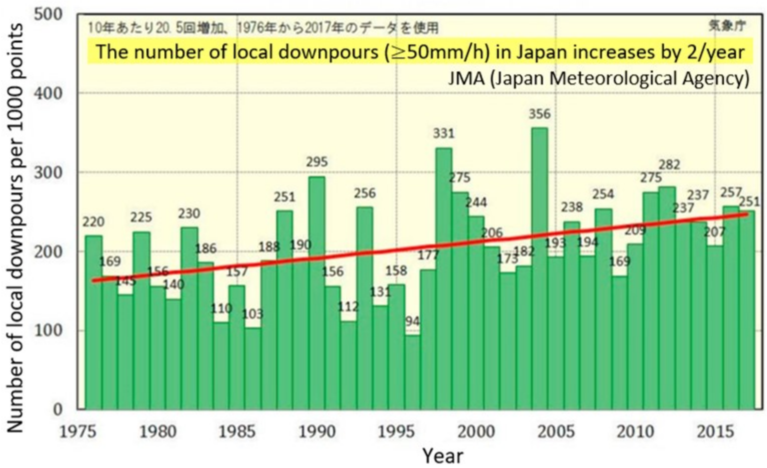

Figure 2. Number of concentrated downpours in Japan (Cabinet Office, Government of Japan, 2018)

Figure 3. Destroyed seawall at Takata-matsubara (Kuwano et al., 2012, 2014).

Figure 4. Reinforced soil walls in Rikuzen-takata City (Kuwano et al., 2012, 2014).

Figure 5. Front view of RSW1 (Kuwano et al., 2012, 2014).

Figure 6. Close-up view of damaged RSW1 (Kuwano et al., 2012, 2014).

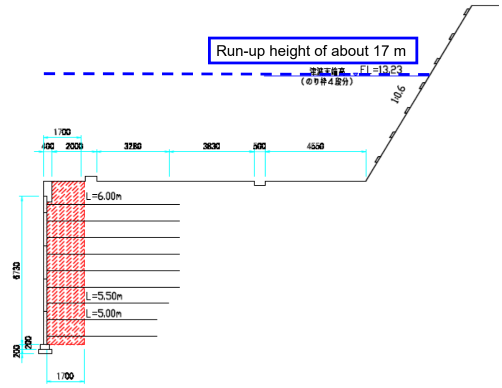

Figure 7 Cross section of RSW1 (courtesy of Dr. Otani, Hirose Corp.) (Kuwano et al., 2012, 2014).

Figure 8 Erosion of the backfill of damaged RSW1 (courtesy of Dr. Otani, Hirose Corp.) (Kuwano et al., 2012, 2014).

2 GEOSYNTHETICS WALLS TO PRIVENT AND MITIGATE HYDRAULIC IMPACT

2.1 *Introduction – Tsunami impact on reinforced soil walls by the 2011 earthquake*

Tsunami was the most serious impact of the earthquake as mentioned before. Inundation height and run-up height were as high as about 40 m (Tsunami Joint Survey Group, 2012). Many seawalls and river dikes were washed out by the tsunami as shown in Figure 3. However, many reinforced soil walls survived the tsunami impact, though they were partly or fully submerged. There are numbers of reinforced soil walls in Tohoku region. Miyata (2012) reported the damage of the walls by the direct impact of the earthquake (shaking) and summarized that just less than 1% of the walls were seriously damaged but more than 90% of the walls did not show any damage. Most of the reinforced soil walls were constructed without considering effects of water. However, some of them were exposed to the direct impact of tsunami. The height of the tsunami by the 2011 Tohoku Earthquake was extraordinarily high. Although some of them were seriously damaged by the tsunami, many of them survived with a little damage. In the followings, some case histories on the reinforced soil walls which were subjected to the impact of the tsunami.

Figure 9 Location of RSW2 (courtesy of Dr. Otani, Hirose Corp.)
(Kuwano et al., 2012, 2014).

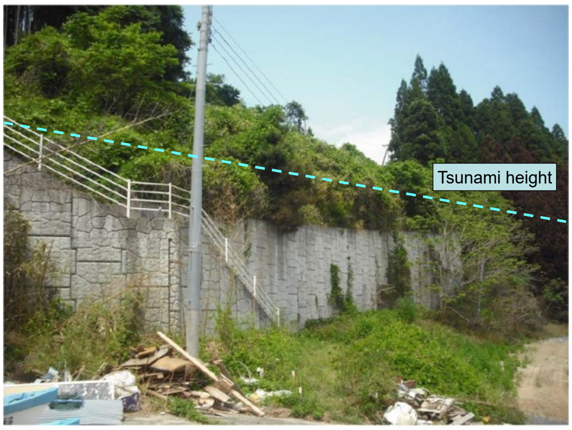

Figure 10 Close-up view of RSW2 (courtesy of Dr. Otani, Hirose Corp.)
(Kuwano et al., 2012, 2014).

Rikuzentakata City is located at the south end of Iwate Prefecture (the northeast of Tohoku region). The main part of the city was washed out by the tsunami with the inundation height of about 15 m, which is almost the height of four to five stories building. About 2,000 people are dead or missing in the city.

Steel strip wall (Terre Armee wall), indicated as RSW1 in Figure 4, with the maximum wall height of 6 m was constructed at the junction of Hirota reclamation dike and the road embankment on the slope. The area was hit and fully submerged by the tsunami with the estimated run-up height of 17 m. Most of the about 500 m long reclamation dike was washed out by the tsunami except the small part which is near the RSW1 side end where the floodgate was located. Figure 5 is the front view of the damaged RSW1. It is seen that the only a part of the wall near the dike is seriously damaged. Figure 6 is a close-up view of the wall. The upper part of the wall collapsed. Many facing panels fell down and the backfill of the wall was lost. Though it is not clearly seen in this figure, the lower part of the wall was also damaged due to the scouring at the footing. Some of the footing members were brought out and part of soil was lost. Figure 7 is a typical cross section of the wall. Although the cross section is ordinary, the depth of embedment was probably about 40 to 50 cm and a bit too small as a coastal structure. It resulted in the damage of the lower part of the wall as mentioned above. However, it is to be pointed out that the most of the damaged part of the RSW1 was covered with the soil of reclamation dike before the earthquake, and probably therefore the footing depth was thought to be enough when the wall was designed. Another and more serious problem with the RSW1 was that the wall was not constructed continuously from the sea side to the land side. It was interrupted at the junction of the wall and the reclamation dike. The soil of the dike was probably washed out by the tsunami first. Then the backfill of the wall was eroded from the interruption of the wall toward the back of facing panels of the reinforced soil wall as seen in Figure 8. Once the backfill was lost, the facing panels and reinforcing members, which used to support the backfill, were not supported by the backfill and the panels fell down. If the wall was constructed continuously without any interruption, damage of the wall is thought to have been much less.

Figure 11 Scouring at the abutment of the Nanakiri overpass （Kuwano et al., 2012, 2014).

Figure 12 Slight damage at the expanded metal mesh facing of RSW3（Kuwano et al., 2014).

Although the steel strip wall (Terre Armee wall), RSW1, was seriously damaged by the tsunami as mentioned above, it is probably not fair to conclude that Terre Armee does not resist tsunami impact. Another Terre Armee wall, RSW2, was located on the east side of the peninsula opposite to RSW1 as shown in Figure 4. The tsunami hit the peninsula from both east and west sides. The RSW2 was constructed on the beach to support the road as shown in Figure 9. The maximum wall height of RSW2 is 10.5 m. The wall was submerged in the tsunami with the estimated run-up height of 14.9 m. However, in contrast to the RSW1, the damage of the RSW2 was negligibly small as seen in Figure 10. There could be two possible primary factors of the small damage. The first one is that the depth of embedment is more than 1.5 m, much bigger than that of the RSW1. Therefore, the backfill of the RSW2 was not lost from the bottom of the wall. The second factor is that the backfill of the reinforced soil wall was fully covered with rigid concrete panels without interruption as seen in the RSW1 which was seriously damaged by the tsunami.

In the downtown area of Rikuzentakata City, Nanakura overpass of Route 340 across the Ofunato railway line was located near the Kesen River, along which the tsunami went upstream besides the invasion from the coastline. As the handrails of the bridge were bent down toward the river, the overpass was fully submerged and the power of tsunami was more from the sea side than the river side. Four reinforced soil walls with the height of about 7.7 m were constructed at the abutments of the bridge. It has expanded metal mesh facing units with layers of geogrids for reinforcement and geotextiles for horizontal drain. Scouring was found at the foundation of the abutment as shown in Figure 11. This scouring and the damage of handrails indicate huge impact of the tsunami on the bridge. However, damage of the walls was very limited, e.g. a small scoop of backfill as seen in Figure 12. Thin vegetation sheets behind the wire mesh facing panels probably protected backfill from erosion by the tsunami.

2.2 *GRS RW with FHR (full-height rigid) Facing for Railways and Roads*

Geosynthetic-reinforced soil retaining walls (GRS RWs) have been constructed for a total length more than 135 km mainly for railways, including high-speed train lines (Tatsuoka et al., 2013). A full-height rigid (FHR) facing is firmly connected to the reinforcement layers when constructed after a full-height wrapped-around GRS wall has been constructed and the major residual deformation of the backfill and supporting ground has taken place. A number of this type GRS RWs performed very well during the 1995 Kobe and the 2011 Tohoku (Great East Japan) Earthquakes. Tatsuoka et al. (2013) and Watanabe et al. (2017) reported application of GRS RW with FHR Facing for railway structures which are expected to have high resistance to flood and tsunami.

A great number of embankments for roads and railways retained by conventional type cantilever RWs along rivers and seashores collapsed by floods and storm wave actions, usually triggered by over-turning failure of the RWs caused by scouring in the supporting ground (Figure 13a: Tatsuoka et al., 2013). Upon

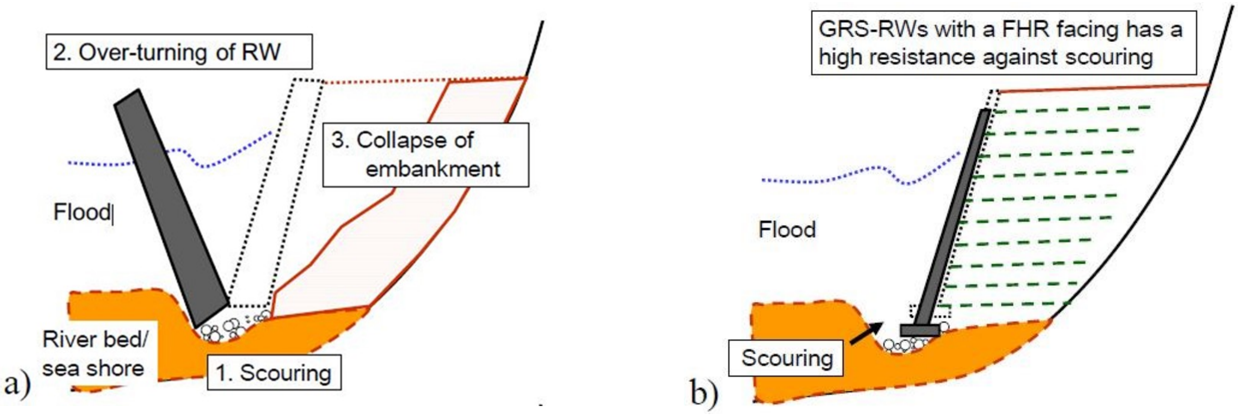

Figure 13 a) Collapse of cantilever RW by scouring in the supporting ground; and b) stable performance of GRS RW with FHR facing (Tatsuoka et al., 2007).

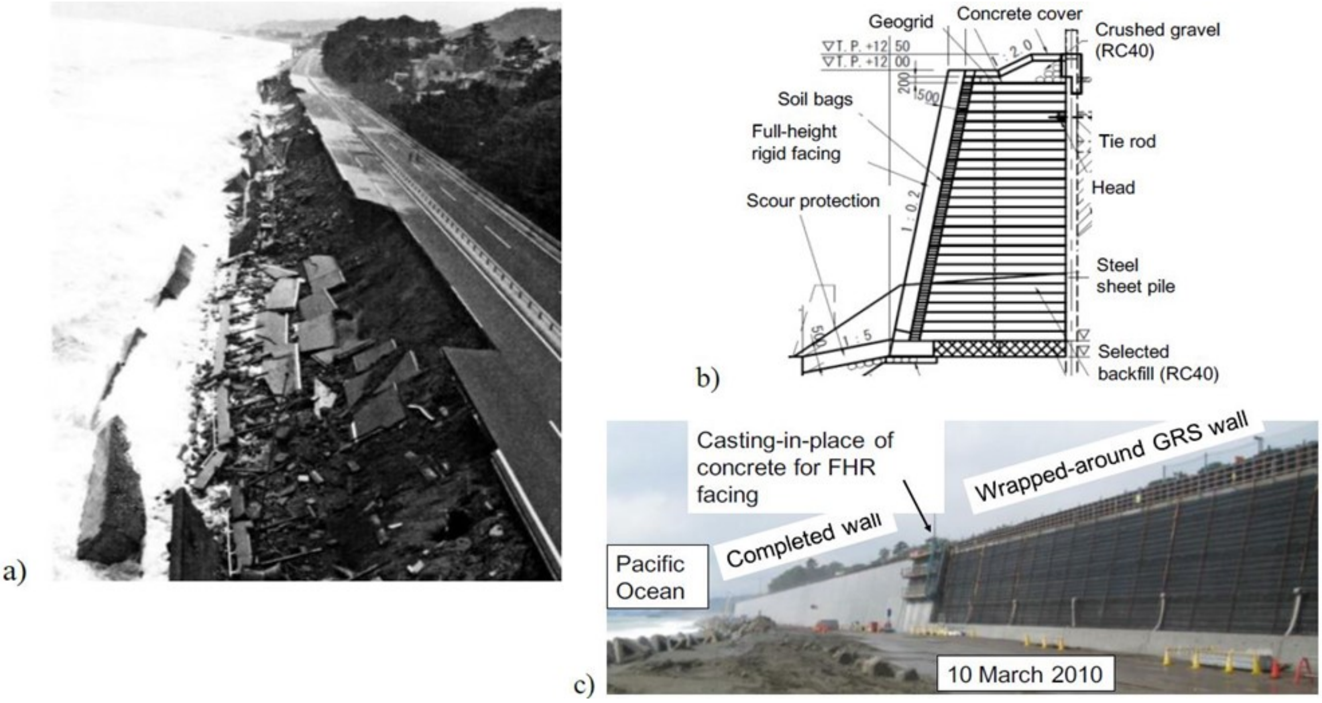

Figure 14 Seawall for Seisho by-pass of National Road No. 1 in Kanagawa Prefecture, southwest of Tokyo: a) collapse for a length of about 1.5 km by Typhoon No. 9, 29th Aug. 2007; b) a typical cross-section of GRS RW; and c) GRS RW under construction (Tatsuoka et al., 2007).

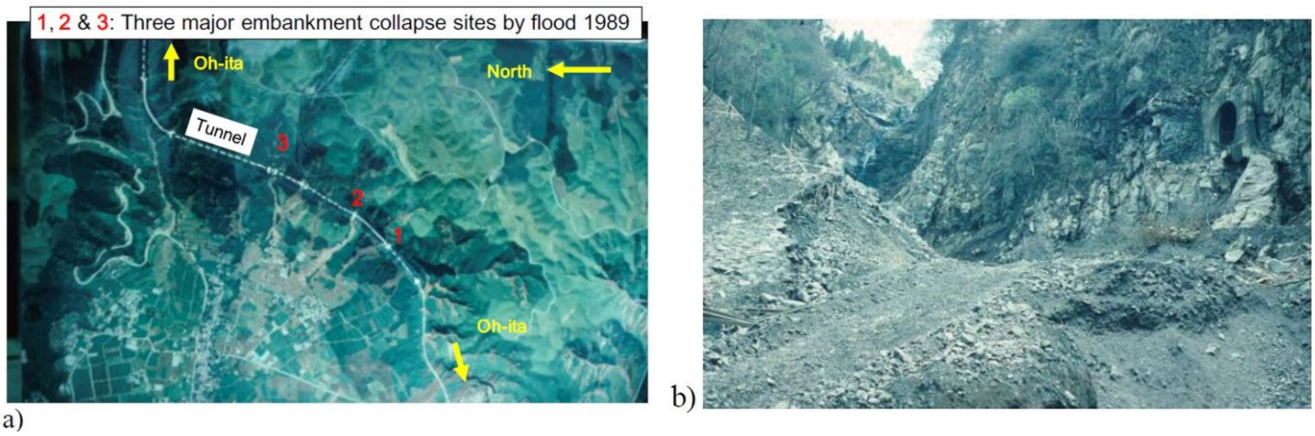

Figure 15 a) Locations of three major embankment failures by heavy rainfall in 1989, Ho-hi Line, JR Kyushu and b) a view from the downstream at site (Tatsuoka et al., 2007).

the collapse of RW, the backfill is quickly and largely eroded, resulting in the close of railway or road. This type of collapse easily takes place, as the stability of a cantilever RW fully hinges on the bearing capacity at the bottom of the RW. On the other hand, GRS RWs with FHR facing is much more stable against the scouring in the supporting ground (Figure 13b). It is particularly important that the facing does not overturn easily and the backfill can survive unless the supporting ground is extremely scoured. As shown in Figure 14a, a large-scale overturning collapse of gravity type RW for a road (Seisho bypass of National Road No. 1) took place for a length of about 1.5 km along a seashore facing the Pacific Ocean. The collapse of the RW was triggered by scouring in the supporting ground, as the mechanism illustrated in Figure 13a, by strong ocean waves during a typhoon No. 9 on 29th Aug. 2007. The wall was reconstructed to a GRS RW with FHR facing (Figures 14b & c). It survives the following storm waves up to now.

A series of railway embankments located in narrow valleys between tunnels in Mt. Aso area in Kyushu Island fully collapsed on 2 July 1989 by floods caused by heavy rainfall (Figure 15). Flood water was trapped back the upstream slope of each embankment due to the clogging of a drain pipe crossing the embankment. The embankments collapsed by over-topping of the flood water. In the downstream, debris flows took place, as seen from Figure 15a, and attacked residential houses at the lower reach. The six embankments were reconstructed by geosynthetic-reinforced embankments, as typically shown in Figure 16, to reduce the amount of earthwork while keeping the stability of embankment to a sufficiently high level.

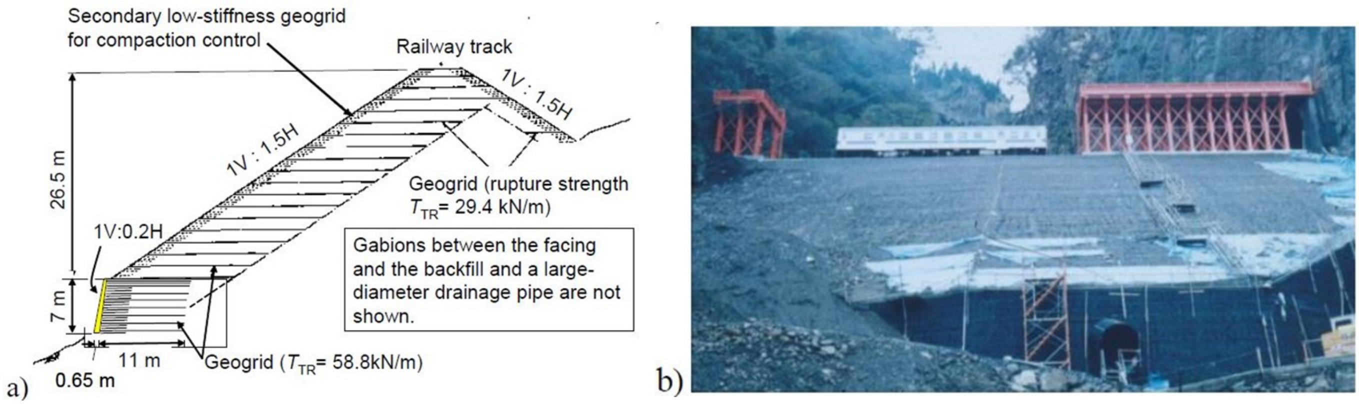

Figure 16 a) Cross-section; b) a view during reconstruction in 1991 of the reconstructed GR embankment. Site 2 of Ho-hi Line, JR Kyushu (Tatsuoka et al., 2007).

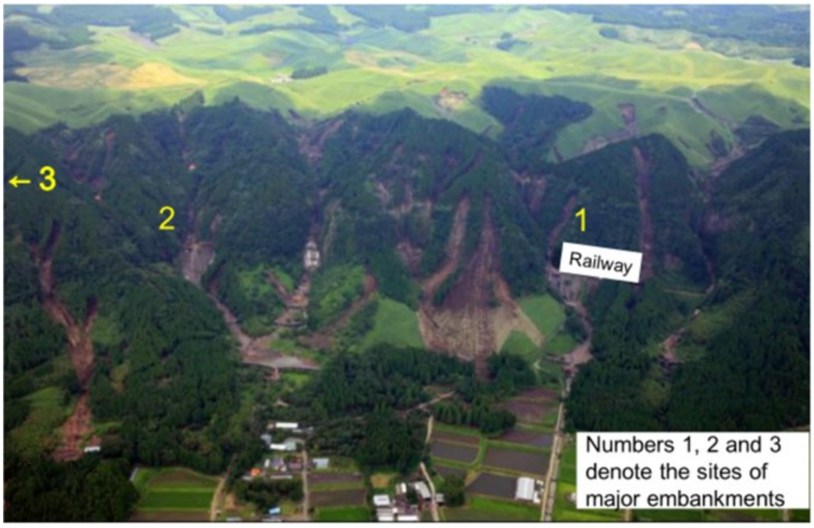

Figure 17. Aerial photograph of Ho-hi Line immediately after the 2012 heavy rain (Tatsuoka et al., 2007).

Figure 18. a) Aerial photograph; and b) a close view from upstream (a & b: immediately after the 2012 heavy rainfall, by the courtesy of JR Kyushu); and c) a view from the downstream; and d) exposed cross-section of geosynthetic-reinforced section (c & d: taken 26 November 2012). Site 2 of Ho-hi Line, JR Kyushu (Tatsuoka et al., 2007).

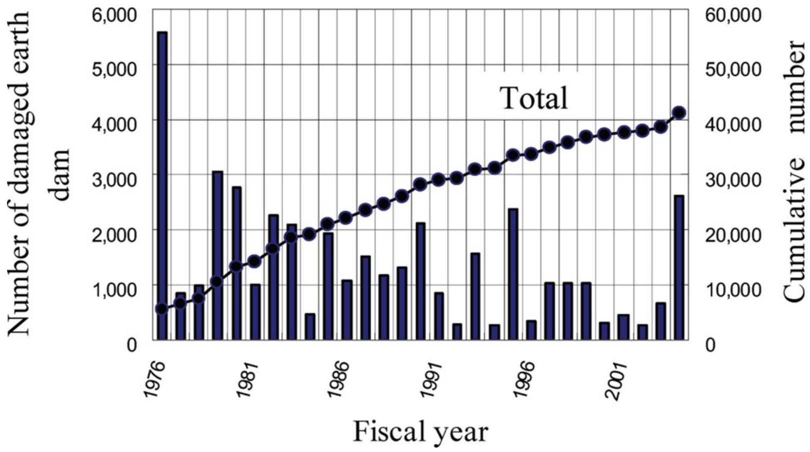

Figure 19. Accumulated and annual numbers of damaged small earth-fill dams in Japan.

To arrange a 3 m-diameter drain corrugate pipe crossing the embankment, a nearly vertical GRS RW with FHR facing was constructed at the downstream toe of each embankment. From 12th to 14th July 2012, 23 years after the first event described above, another, more severe rainfall attacked these sites (Figure 17). The total precipitation during a period from early morning 12 July till evening 14 July reached 816.5 mm with a peak of 500 mm in 5 hours and 106 mm/hour, which was much more intense than the 1989 heavy rainfall with a total precipitation of 650 mm and a peak of 67 mm/hour. A number of embankments that did not collapse by the 1989 heavy rainfall were seriously damaged or totally collapsed by scouring, erosion by over-topping flood and seepage flow of rain water likely with a loss of suction followed by the development of positive pore water pressure. The three major geosynthetic-reinforced (GR) embankments that were reconstructed in 1991 were attacked by over-topping flood due to clogging of the 3 m-diameter corrugate drain pipes by mudflow from the upper reach. However, the main body of these GR embankments survived having been only partially eroded, despite that they were not designed against such over-topping flood. At the site 2 in Figures 15 and 17, the left-hand part (Oh-ita side) of the embankment located between two tunnel exits was unreinforced backfill that survived the 1989 flood and remained unchanged. This part was severely eroded by the overtopping flood of the 2012 rainfall (Figure 18). Figures 18c shows the eroded part of the unreinforced embankment after having been excavated to some extent for restoration works. On the other hand, the right-hand part (Kumamoto side) of the embankment seen in Figure 18a is located at the deepest place of the valley. This part was fully eroded by the 1989 flood and reconstructed with a GRS structure (Figure 16). The exposed cross-section of the GR embankment is shown in Figure 18d. This part of GR embankment performed very well during the 2012 heavy rainfall: i.e., it may be seen from Figure 18c that only some surface layer of the downstream slope of GR embankment was eroded. Although relatively deep gullies were formed in the unprotected downstream slope of the GR embankment, these gullies did not further develop due likely to the resistance of geogrid layers against erosion.

Railway embankments suffered from extensive damage from the tsunami caused by the 2011 Tohoku earthquake and the operations of railway lines were suspended for a long time. Although numerous studies have been conducted on enhancing the earthquake resistance of embankments, studies on resistance against prolonged Tsunami overflows have been insufficient. Therefore, the effect of earthquake prior to the onset of a tsunami as well as the durability of both conventional type and geotextile reinforced type embankment against overflowing are evaluated through the model tests by Watanabe et al. (2017). It will be reported later.

2.3 *Small Earth-fill Dams for Agricultural Irrigation*

In Japan, there are more than 210,000 small earth-fill dams for agricultural irrigation, and almost all are located near cities (Mohri et al., 2007). They must withstand two extreme events. i.e. major floods due to heavy rainfall and earthquakes. These reservoirs have been maintained by local management organizations for some 200 years, but at least 20,000 sites are deteriorating with age such as leakage and sliding. As the body of the dam consists of soil materials, there is a possibility that slight erosion on the slope of the dam caused by rainfall may gradually develop into a largescale collapse. In addition, it has been reported in many papers that a dam body damaged by an earthquake unexpectedly failed.

Figure 19 shows the cumulative and annual numbers of damaged small earth-fill dams in Japan, from 1976 to 2004. The figure shows that complete dam failure occurs several times a year, but most small

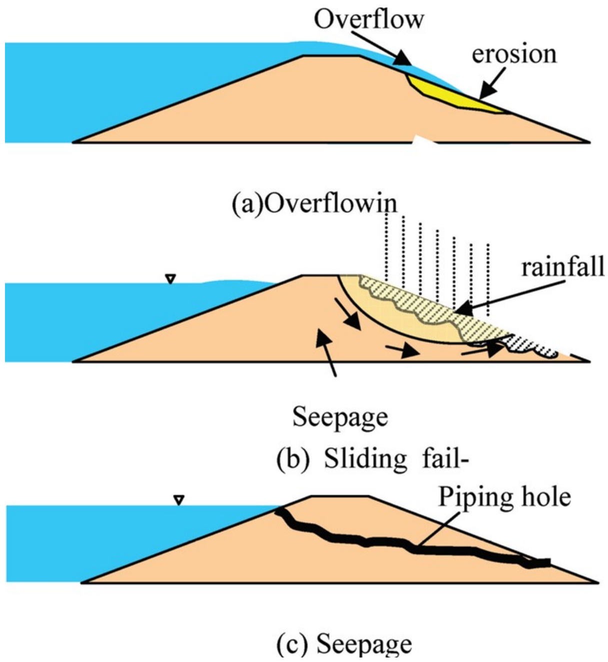

Figure 20. 3 Dam failure modes by heavy rainfall (Hori et al., 1997)

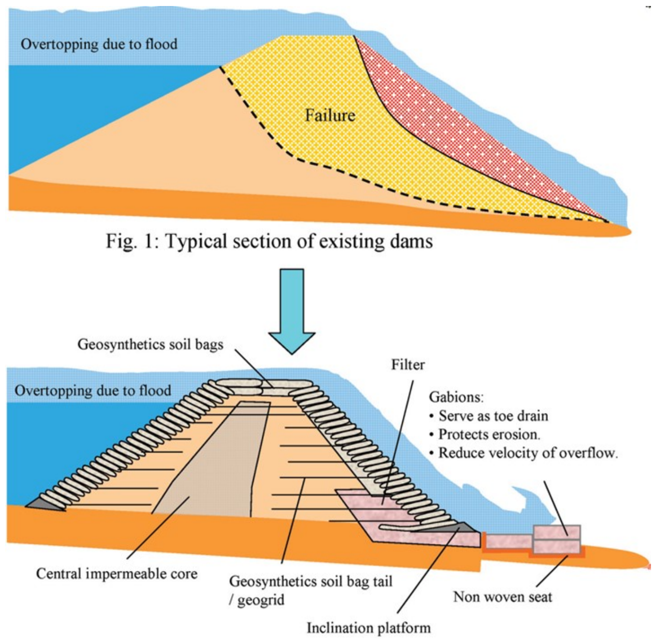

Figure 21. New technology to rehabilitate existing old earth-fill dams to have a high flood discharge capacity (Mohri et al., 2005)

earth-fill dams have been damaged by sliding and leakage. It is obvious that many dams were damaged by earthquakes in 1995 (Kobe) and in 2004 (Niigata-ken Chuetsu), but most of the dams were affected by embankment landslide and overflow caused by rainfall. These small earth-fill dams damaged by earthquakes and heavy rainfall are usually reconstructed to the original condition and structural type, even if the reconstructed earth fill dams may suffer the same damage again when subjected to an earthquake or rainfall of the same level. However, localized downpours exceeding 100 mm/hour and 500 mm/day often occur in Japan recently and sometimes cause unexpected floods. Therefore, it is essential to develop a small earth-fill dam of high durability. The Institute for Rural Engineering of NARO (The National Agriculture and Food Research Organization) made a challenge to develop a small earth-fill dam resisting earthquakes and overflow (Mohri et al., 2007). The challenge was before the tsunami of the 2011 Tohoku earthquake.

Small earth-fill dams have several destruction patterns due to heavy rain. Here, the main causes of destruction can be classified into three types as shown in Figure 20, i.e. failure by overflow, failure by sliding and failure by internal erosion. Existing old earth-fill dams consist of an earth embankment and a concrete spillway. When such dams are designed, additional seismic force due to earthquakes is usually not taken into consideration. In addition, since almost all old earth-fill dams were constructed before the establishment of design standard for spillway capacity, many dam spillways have insufficient capacity to discharge the water of occasional floods. A great number of small earth-fill dams for agricultural irrigation have been seriously damaged or completely failed by overflowing caused by torrential rain of a typhoon and/or a weather front. This natural hazard of overflowing and associated dam failure can totally destroy downstream city areas. For example, the failure of Fujinuma dam, 18 m high irrigation dam, failed completely by the 2011 earthquake and the following overflow. It caused the flood in the downstream to wash away five houses and kill eight people. Therefore, a new method for constructing small earth-fill dams which can tolerate overflowing due to flooding and the seismic forces of earthquakes is needed.

It is very expensive to increase the drainage capacity of a flood discharge spillway system of a reinforced concrete (RC) structure so that it can discharge the design flood that might take place once every 200 years. Moreover, a large spillway system on a small earth-fill dam requires reinforcing the dam dike itself in order to increase the stability of the dam. This rehabilitation approach is not cost effective and needs too long time. Mohri et al. (2005) proposed protecting the downstream slope of such earth-fill dams by using soil bags anchored with geosynthetic reinforcement layers arranged inside the slope as shown in Figure 21. This is a realistic, cost-effective and quicker method to rehabilitate a great number of old earth-fill dams without increasing the capacity of an existing flood discharge RC structure. Moreover, the slope constructed or reconstructed by the new technology is more stable against seismic load. In the new construction method, the dam section is a composite structure of earthwork, impermeable core zone, geosynthetic soil bags with extended tail (GSET) filled with appropriate backfill material and

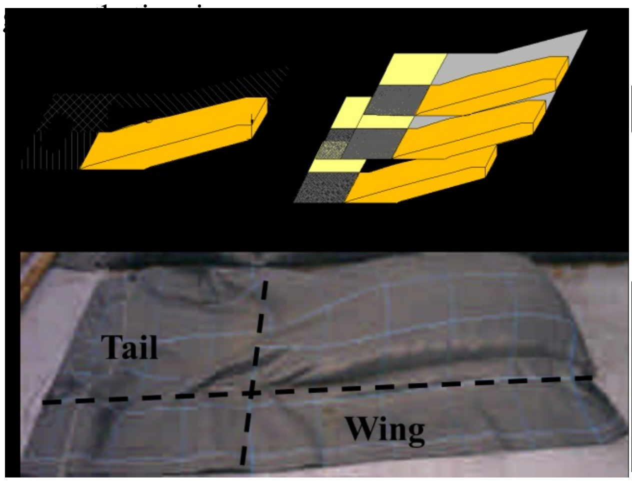

Figure 22. GSET (Geosynthetic soil bag with extended tail) and inclined stacking system (Mohri et al., 2007).

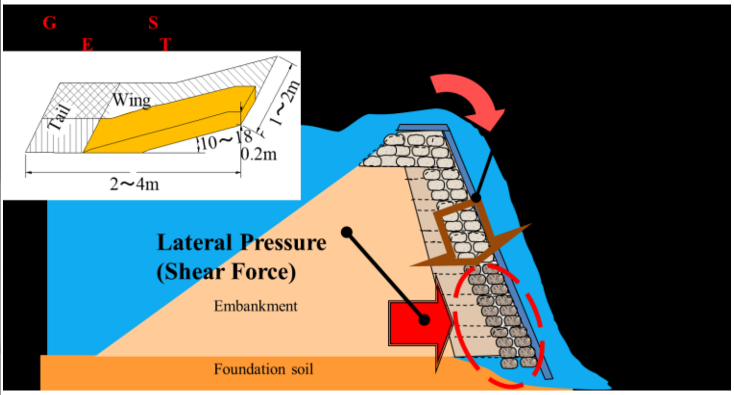

Figure 23. Research focus points for soil bag system

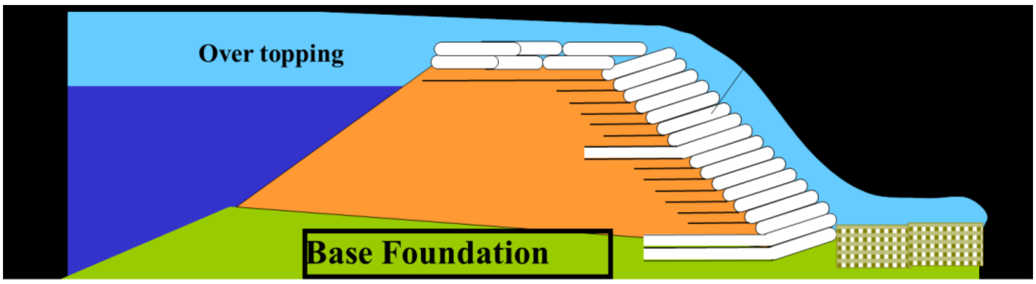

Figure 24. Modified dam section incorporating GSET slope with inclined soil bags.

(Figure 22). The use of advanced soil bags not only increases stability against overflowing but also provides resistance against earthquake-induced forces. Research focus points are summarized in Figure 23.

GSET is a method for piling up soil bags as shown in Figure 9 to construct an earth-fill dam that has higher stability even when a flood overflows its embankment. This soil bag, which has a flat shape with an aspect ratio of 5 to 8, consists of a large soil bag with a mass of 200 kg or more, and a tail and a wing that are connected to this soil bag. The wing is inserted between neighboring soil bags, thereby ensuring the strength of stacked soil bags serving as a potential wall. The tail is installed within the embankment, so it exerts a reinforcement effect in combination with stacked soil bags and embankment. Namely, the body of the soil bag system and the tail reinforce a wider area of the embankment, and increase the strength of the whole body as a flexible wall. Furthermore, as the materials within the soil bag are confined by the bag and exert a larger bearing capacity, on-site soil of low quality can be used. When high-permeability materials such as crushed stone are used for the embankment, its stacked layer can also serve as a drain. Therefore, these materials provide resistance to overflow and also improve measures against leakage, and the safety of the dam during an earthquake increases. It is important to make clear the soil bag strength and full use of the capability of the soil bag system in order to stabilize the structure of stacked soil bags. However, It is difficult to ensure sufficient resistance by simple stacking because sliding friction between soil bag materials is small and its friction dominates the shear deformation of the whole stacked body. For this reason, Matsushima et al. (2006) suggested a method to increase the shear resistance of the body by installing soil bags at a inclined angle, and provided detailed data on the increased resistance. Figure 24 indicates a modified dam section incorporating GSET slope with inclined soil bags.

Half-scale model tests were conducted in a laboratory flume to develop the advanced soil bag system with full-scale soil bags. A 4.5m high embankment model with soil bags used for an actual earth-fill dam was constructed in the flume to conduct an overflow test. The overflow depth was gradually increased from about 0.2 m to 0.6 m for a few hours in each step. Deformation of the embankment and damage of soil bags were observed. This model had a 2.3 m high downstream slope with V:H=1:1.2. Kasama sand (ρ_s=2.650g/cm^3, ρ_{dmax}=1.935, w_{opt}=11.6%) and fine-grained fraction mixed materials (ρ_s= 2.617g/cm^3, ρ_{dmax}=1.470, w_{opt}=24.6%, Kanto loam 1: Kasama sand 1.5) were used for the embankment and for the core soil, respectively. As shown in Figure 25, soil bags were stacked on the upstream and downstream faces of the embankment model to construct a surface that is resistant to overflow. These soil bags were stacked

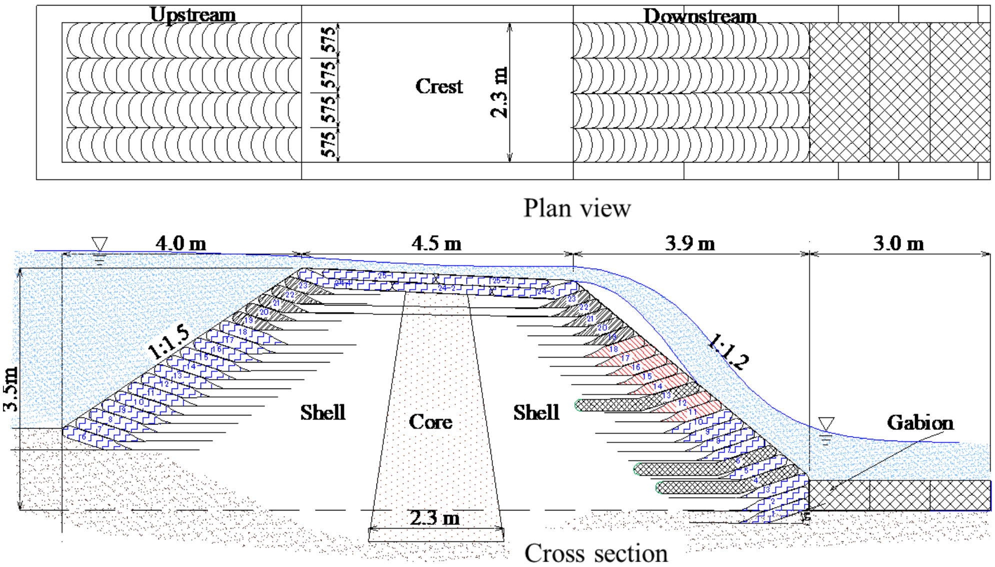

Figure 25. Model test embankment in laboratory flume.

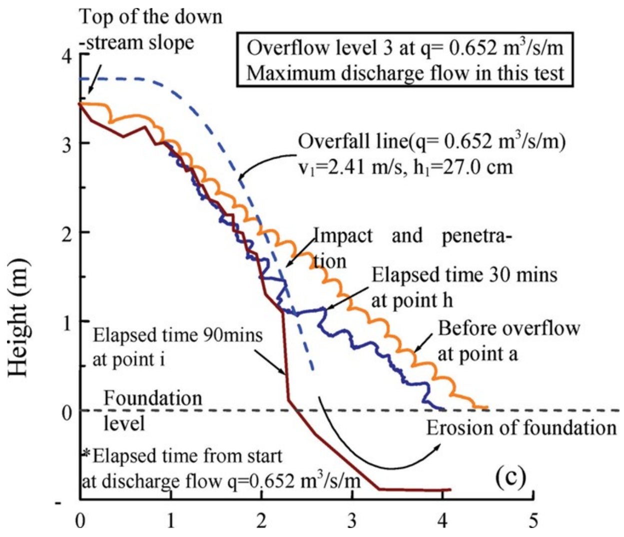

Figure 26. Lateral displacement of soil bag surface after overflowing tests (Mohri et al., 2007).

Figure 27. Eroded surface of Soil bags

with an angle of 15° to the foundation ground in order to increase the shear resistance of the stacked soil bags and enhance the safety of the model. Referring to the results obtained through a compression test, recycled crushed stone (RC40) was used as an infill material for the soil bags to improve the strength, and to enhance overall safety of the embankment model. PP sheet having tensile strength of 1.25kN/m and tensile strain of 29.8% was used for the soil bag material. Unlike a normal large soil bag, this soil bag basically has a flat shape with a large aspect ratio (L/H=5–8). As shown in Figure 22, the soil bag has a wing and a tail at its side and rear end, respectively. The wing is inserted into neighboring soil bags to prevent separation between soil bags, and also to help the whole soil bag system to serve as a wall similar to a reinforced earth retaining wall because the tail is buried in the embankment.

The flow rate was gradually increased from Step 1 to Step 7. Overflow water with a low flow rate went along the surface of the soil bag and was basically in the state of nappe flow, however, a small hydraulic jump occurred on each soil bag steps. In Steps 2 and 3, the overflow ran down the downstream slope of the embankment with the strong entrainment of air and entered a state of skimming flow. As a result, the running water started to separate from each soil bag surface, resulting in more sand being sucked from the soil bags. From Step 4, the water's flow velocity increased more, causing a hydraulic jump at the crest. Figure 26 shows the lateral displacement of soil bag surface after overflowing tests.

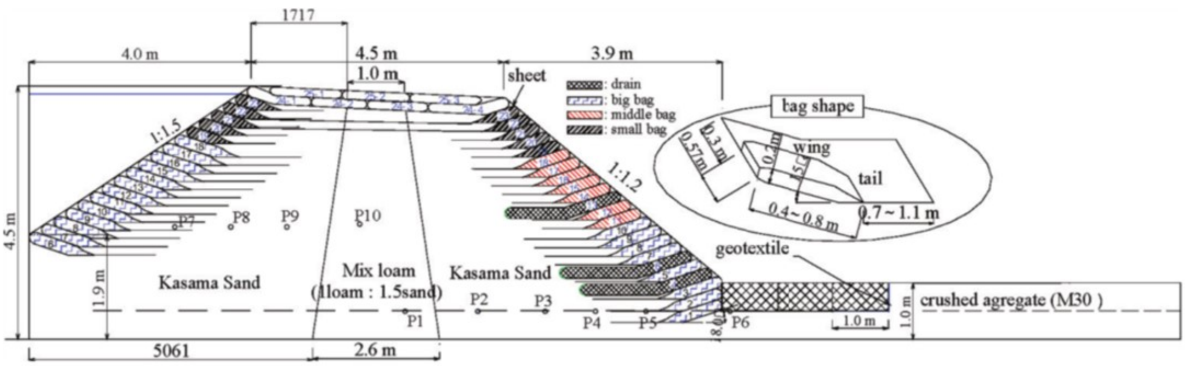

Figure 28. Cross section of a full-scale field model earth-fill dam (Mohri et al., 2007).

Figure 29. Overflow test of spillway of the full-scale field model earth-fill dam.

In Steps 1, 2 and 3 with a low flow rate, only limited amount of soil leaked from the soil bags. In Steps 4 and 5, as shown in Figure 27, fill materials in the soil bags were discharged, so their surface sank. This phenomenon of washout occurred uniformly across the downstream slope of the embankment, but it was centered in the area where overflow water jumped from the crest landed. For Step 6, considering damage and deterioration of soil bag materials, artificial damage was given to the soil bags at the interface between the soil bags' surface and running water to continue this test. As the damage expanded, some of the fill materials were discharged. Thereafter, however, the bag materials covered the upper fill materials again and adhered tightly to the whole surface of the embankment, so the overflow water did not erode the embankment's materials directly, resulting in no overall collapse of the dam. In Step 7 ($1.5m^3/s$), where water with a higher flow rate flowed continuously, a soil bag on which the overflow water landed directly broke, causing the successive destruction of lower soil bags. However, the lower part of the embankment did not deform further, and destruction of the whole dam did not occur. Based on these findings, it was demonstrated that GSET-dam had great resistance to piping and suction and remained stable without complete collapse against large overflow. In addition, it is effective to place materials such as soil-cement and vegetation on the surface of the soil bags to ensure the durability of small earth-fill dams.

NARO constructed a full-scale earth-fill embankment using GSET as shown in Figure 28, examined its construction performance, observed its behavior during and after the construction and conducted a test to evaluate the long-term durability of the model. For this demonstration test, an embankment with a height of 3.2m, an upstream slope of V:H=1:1.5, a downstream slope of V:H=1:1.2 and a body width of 21m, in which 10 m of embankment was constructed with soil bags containing recycled crushed rock (RC-40), and 11 m was constructed with soil bags containing Kanto loam. In this field model test, the embankment was overlaid with soil-cement and vegetation to confirm the effectiveness of these methods of preventing UV deterioration of soil bags in the final stage. Overflow test of spillway of the full-scale field model earth-fill dam was carried out as shown in Figure 29 and proved high resistance of GSET-dam to overflow.

Figure 30. Tsunami and damage of coastal dike at Tofugaura in Iwate Prefecture.

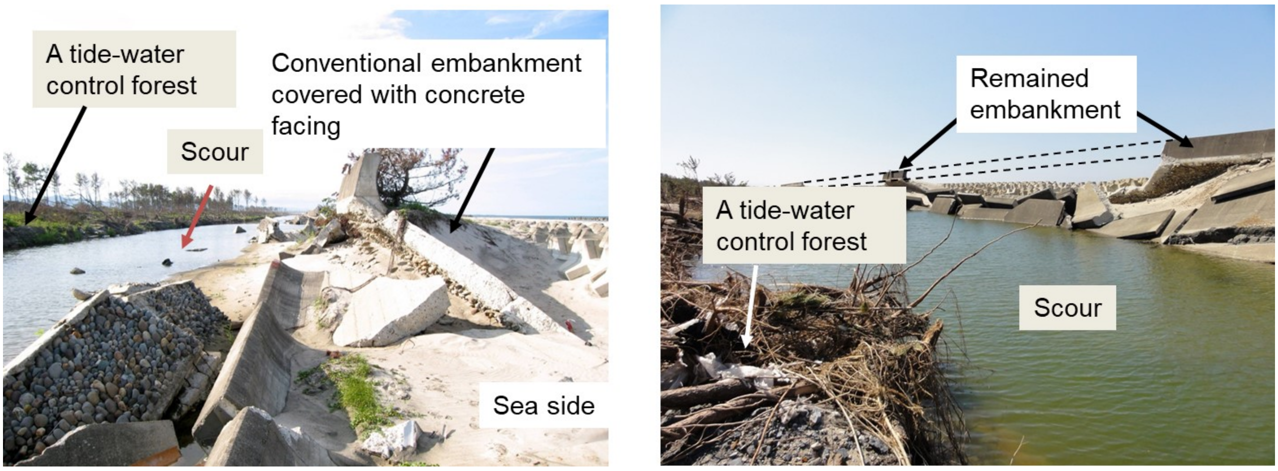

Figure 31. Damage of coastal dike and its surroundings.

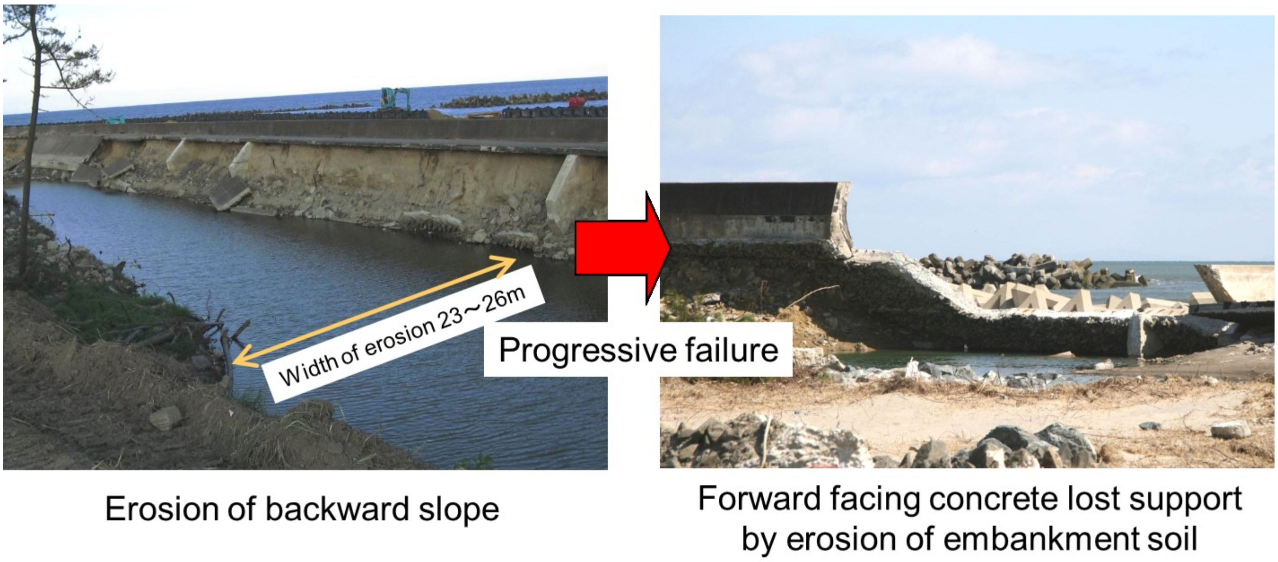

Figure 32. Possible sequence of coastal dike failure.

2.4 *Geotextile-reinforced levee against Tsunami*

After the devastating damage of tsunami caused by the 2011 Tohoku earthquake, Japan Chapter of IGS (JCIGS) established "Committee for Development of Geotextiles Reinforced Levee against Tsunami" in 2012 to propose a geotextiles reinforced levee persevering in resisting tsunami attack. The committee published "Manual for Design and Execution for Geotextiles Reinforced Levee against Tsunami - Proposal-" in 2014. The manual contains five chapters, i.e. overview, investigation, design, construction and maintenance. Knowledge and experience of the Japan Chapter, e.g. the GSET-dam and the GRS RW with FHR which are introduced in this report, were compiled in the manual.

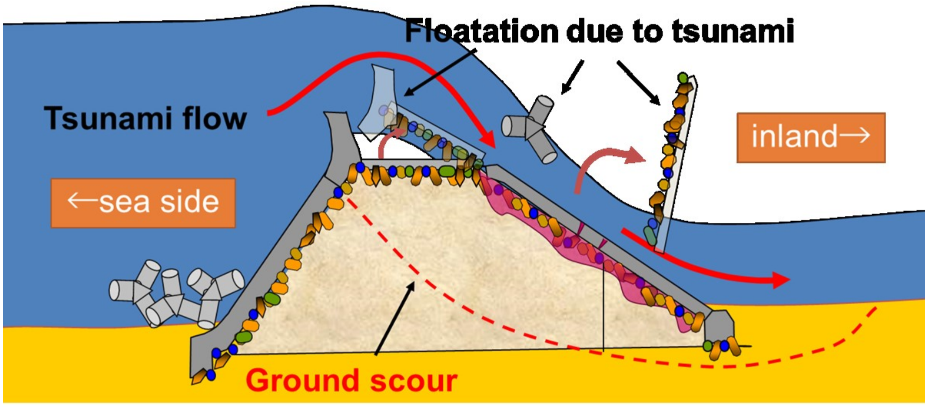

Figure 33. Sequence of coastal dike failure.

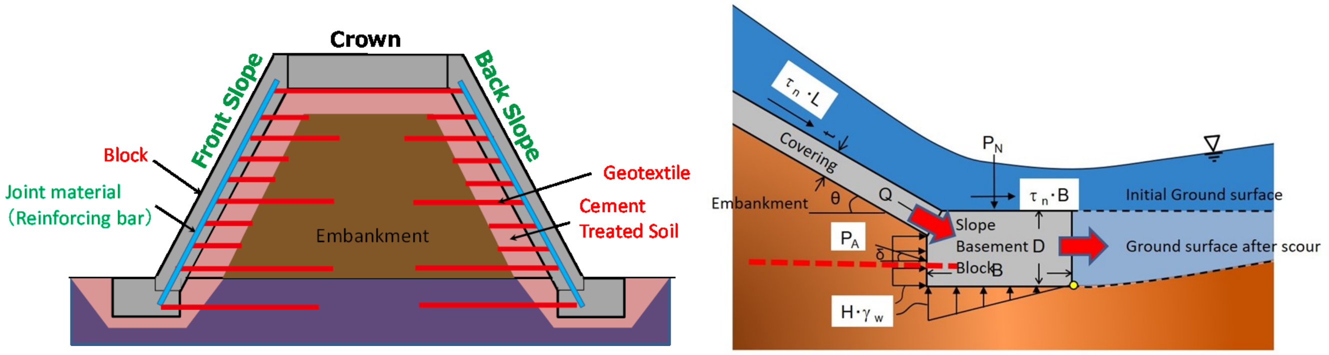

Figure 34. Proposed cross section of GR-levee.

The manual summarized damage of coastal levees and their weak points. Almost 20,000 people are dead or missing by the 2011 Tohoku earthquake. Tsunami was the most serious impact of the earthquake. Tsunami Joint Survey Group (2012) reported that inundation height and run-up height were as high as about 40 m. It killed thousands of lives and caused extensive damage of various structures such as seawalls and bridges. Many seawalls (coastal dikes) and river dikes were washed out by the tsunami Kuwano et al. (2012, 2014). An example of tsunami impact on coastal dike is shown in Figure 30. Figure 31 shows destroyed coastal dike of conventional embankment covered with concrete facing and its surroundings such as scour and overturned concrete facing. Figure 32 indicates a possible sequence of seawall failure, i.e. erosion on the backward side followed by collapse of the forward side concrete facing due to the loss of supporting embankment soil. Weak points of conventional seawall against tsunami are summarized in Figure 33, showing that the overflowing tsunami attacked the coastal dike and tore the concrete facing out of the back slope, then the embankment soil was eroded and finally the forward side concrete facing collapsed due to the loss of supporting embankment soil. Cracks and separations of concrete facing triggered the abovementioned failure sequence of coastal dike.

Proposed cross section of GR-levee for a strengthened coastal dike is shown in Figure 34. To avoid cracks and separations of concrete facing, deformation of the embankment should be reduced even for strong earthquake by geotextile reinforcement. As another benefit of using geotextile, steep slope can be constructed. Concrete facing panels and blocks which covers the slopes and crown should be connected strongly to reduce the gap between them. It improves the safety against detachment of covering facings. To sustain the safety of the back slope, scour of the foundation ground should be reduced as it causes the loss of embankment soil from the bottom of the slope. Slope basement block should be to increase resistance to scour of back side ground. Scouring of ground back of the foundation causes failure of basement block failure by loss of passive earth pressure, sliding of covering block, and the gap made at the top of the slope causing erosion of the embankment.

Figure 35 shows example of GR-levee (seawall). Cement treated soil is used at the surface of soil embankment to reduce the erosion. Facing blocks are connected tight with reinforcing bars to prevent facings from being detached. Whole the components of GR-levee are combined with layers of geotextiles. As the GR-levee can make a steeper slope, 1:0.5 for example, as compared to the gentle slope of conventional dike, 1:2.0 for example. It means the GR-levee can be higher than the conventional type coastal dike for the same land width. Model GR-levees of gentle slope type and steep slope type were constructed successfully as shown in Figure 36.

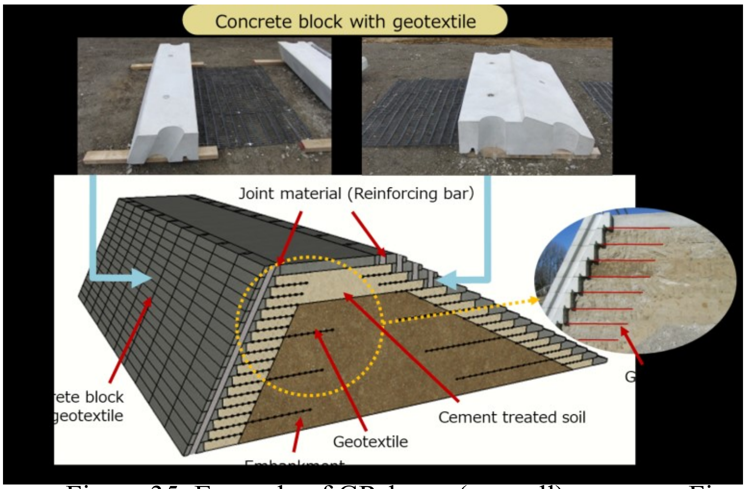

Figure 35. Example of GR-levee (seawall)

Figure 36. Construction of model GR-levees of gentle slope type and steep slope type.

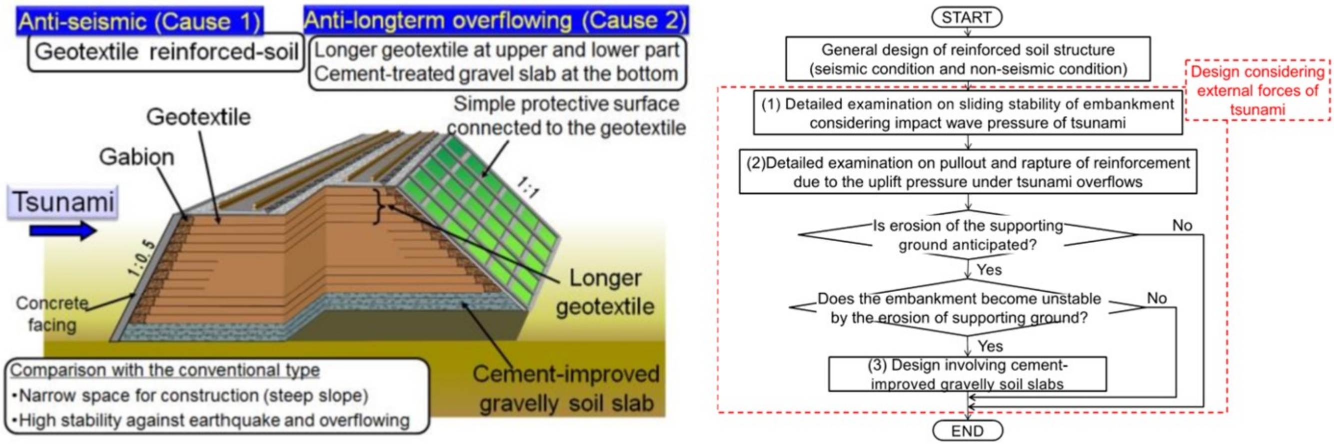

Figure 37. New geotextile reinforced-soil embankment for railway and design flow of the embankment structure considering tsunami effect proposed by RTRI (Watanabe et al., 2017).

2.5 *Application of geosynthetics reinforced soil structure to railway and river dike*

Railway embankments suffered from extensive damages from the tsunami triggered by the 2011 Tohoku earthquake. Several studies have been conducted to enhance the earthquake resistance of railway embankments based on critical damages caused by Hyogo-ken Nanbu Earthquake (Kobe earthquake) in 1995. This critical damage as well as precise investigation after the earthquake led to the wide application of geotextile reinforced soil structures (hereinafter referred to as the "reinforced soil structure") such as "RRR Construction Method" developed by the Railway Technical Research Institute. However, there have been few studies related to enhancing the tsunami resistance of railway embankments, and there is a need for an optimum restoration method for railway embankments vulnerable to tsunamis. In the current design standard for Japanese railway structure, the required performances and performance indices under seismic and non-seismic conditions are clearly defined, however, required performance of railway structure against tsunami actions is not defined. Furthermore, since the railway embankments in coastal areas are generally constructed on the inner side of coastal levees, the railway embankments are often expected to become the secondary barriers (multiple protection) against prolonged overflows of tsunami. In view of above, it is important for railway embankment to exhibit sufficient stability and ductile behavior against tsunami, in a similar way to coastal levees.

The Railway Technical Research Institute conducted an analysis based on onsite surveys as well as wave model experiments and concluded the primary causes of the damages. RTRI proposed a new geotextile reinforced-soil embankment for railway and design flow of the embankment structure considering tsunami effect (Watanabe et al., 2017) as shown in Figure 37.

River levee breach is another natural disaster from which Japan has been suffered repeatedly. On September 10, 2015, an extreme flood due to heavy rain, exceeding 500 mm/day, of typhoon No. 18 caused a

Figure 38. Levee breach in Kinugawa River was caused by extreme flood due to typhoon No. 18.

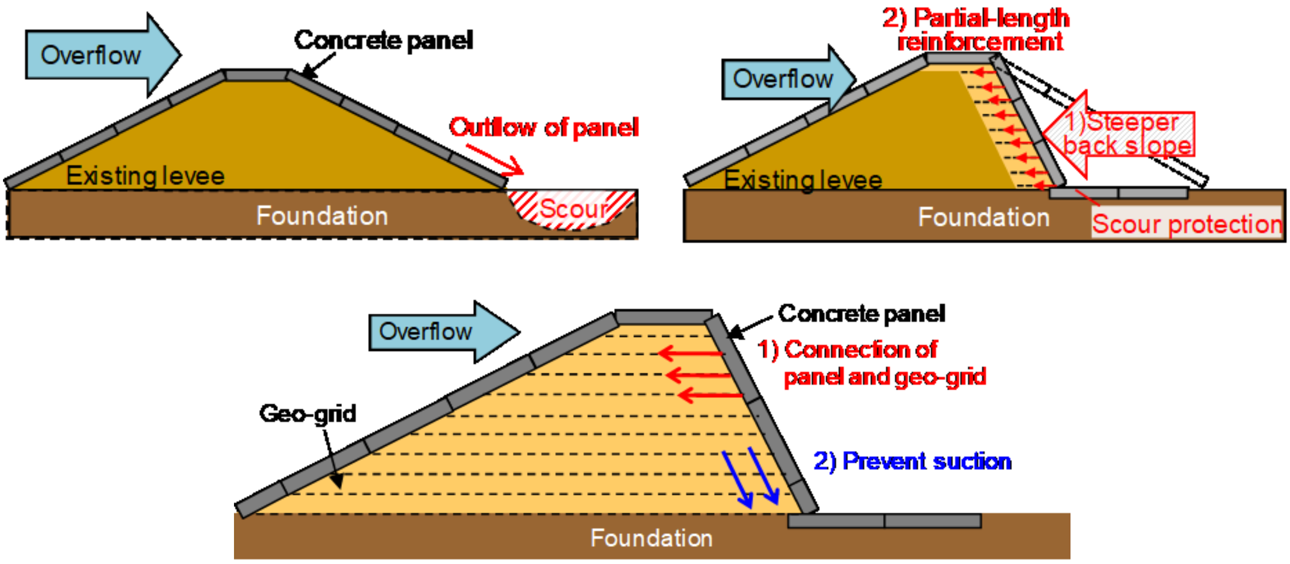

Figure 39. Ordinary armored levee, GRS levee with partial length reinforcement, and GRS levee with full-length reinforcement (Kurakami et al. 2016b).

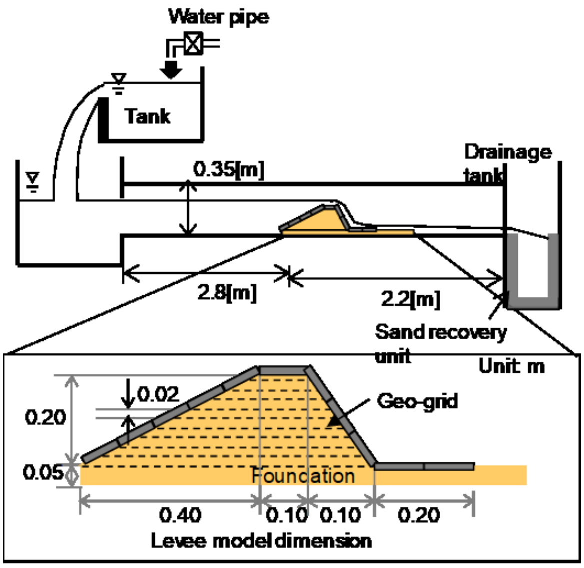

Figure 40. Schematic illustrations of the open channel used in overflow model tests and cross-sectional shape of the levee model (Kurakami et al. 2016b).

levee breach in Kinugawa River, Japan as shown in Figure 38. This breach was mainly due to overflow and resulted in extensive flood damage in Joso City, Ibaraki Prefecture. Levee failures have occurred in a number of places globally and have caused severe damage along rivers. River levees are generally designed to protect against scour, infiltration, and earthquakes for water levels below the designated high water level (HWL), and hence overflows exceeding the HWL are not generally considered for the design of river levees. Earthen levees made up of sediments, including sand and clay, are typically found in the world because river levees are originally semi-natural structures made of sediments transported from upstream regions of the river. However, earthen levees have the potential to fail due to overtopping flows. Armored levees, which are covered with concrete panels, have been introduced to reinforce the levee against overflow erosion, though such levees can still collapse due to overflow erosion when the panels are swept away by the current created by a flood. The development of a new reinforcement technology for a river levee to withstand floods and earthquakes is needed.

To increase the resistance of armored levees against overflow erosion, a river levee with geosynthetic-reinforced soil, called a GRS levee, was proposed by Kurakami et al. (2016a, b). In a GRS levee, the concrete panels are connected to geo-grid layers reinforcing the levee material as shown in Figure 39. A series of tests (Figure 40) to evaluate the resistance of the GRS levee to overflow erosion was carried out and it showed that the GRS levee can survive prolonged overflow conditions.

3 OTHER APPLICATIONS OF GEOSYNTHETICS

Besides the use of geosynthetics to prevent and mitigate hydraulic impact as a reinforced soil wall, geosynthetics are used for mitigating natural disasters such as coastal protection by erosion control with geotextile tubes (Lawson, 2008) and rockfall prevention works.

The erosion control performance of sand-packed geotextile containers, which were installed on the Miyazaki coast, was investigated in Japan (Murakami et al., 2015, Mitsui-sanshi, 2018). The coast is backed by eroding sand dune with 8 to 12 m height formed alongshore for a total of 7 km coastal stretch. For the purpose of dune erosion control, a series of containers was buried alongshore at the foot of dune for 2 km coastal stretch in 2013, which were exposed to typhoon waves. Significant erosion was observed by typhoon waves in unprotected areas while no erosion was observed in the areas protected by containers although some containers were damaged by severe foreshore erosion.

Geosynthetics are used also for rockfall prevention works, e.g. Geo-rock wall (Maedakosen, 2018), with the combination of reinforced soil wall and soil bags. As soil is a flexible material and shows highly plastic deformation, it can absorb the energy of rockfall properly.

4 SUMMARY

Geosynthetics technology is used for preventing and mitigating natural disaster. Various challenges have been made in Japan. Some examples of such challenges are introduced in this report.

ACKNOWLEDGEMENT

This report was made by summarizing the works done by past and present members of Japan Chapter of IGS. Their contribution should be highly appreciated.

REFERENCES

Cabinet Office, Government of Japan. 2018. Bousai-hakusho (White paper for disaster prevention) 2017. http://www.bousai.go.jp/kaigirep/hakusho/pdf/H30_fuzokusiryo1.pdf, viewed on August 10, 2018.

Committee for Development of Geotextiles Reinforced Levee against Tsunami, Japan Chapter of IGS. 2014. Manual for Design and Execution for Geotextiles Reinforced Levee against Tsunami -Proposal-. Japan Chapter of IGS

Kurakami, Y., Nihei, Y., Morita, M., Futami, S. & Itakura, M. 2016a. Effect of river levee with geosynthetic-reinforced soil against overflow erosion and infiltration. Proc. 6th International Symposium on Hydraulic Structures, Portland, USA.

Kurakami, Y., Nihei, Y., Ooyama, M., Morita, Kikuchi, Y. & Tatsuoka, F. 2016b. Laboratory experiments on resistance of river levee with geosynthetic-reinforced soil against overflow erosion. Proc. 6th Asian Regional Conference on Geosynthetics - Geosynthetics for Infrastructure Development, New Delhi, India.
Kuwano, J., Koseki, J. & Miyata, Y. 2012. Performance of reinforced soil walls in the 2011 Tohoku Earthquake, Proc. 5th Asian Regional Conference on Geosynthetics (GeosyntheticsAsia2012), Bangkok, Thailand, pp.85-94.
Kuwano, J., Miyata, Y. & Koseki, J. 2014. Performance of reinforced soil walls during the 2011 Tohoku Earthquake, Geosynthetics International, Vol.21, No.3, pp. 179-196. DOI=http://dx.doi.org/10.1680/gein.14.00008
Lawson, C.R. 2008. Geotextile containment for hydraulic and environmental engineering. Geosynthetics International, Vol. 15, No. 6, pp. 384-427.
Maedakosen. 2018. Geo-rock wall. http://www.maedakosen.jp/mdk/construction/slope-disaster/georock.html, viewed on August 12, 2018. (in Japanese)
Matsushima, K., Aqil, U., Mohri, Y., Tatsuoka, F., & Yamazaki, S. 2006. Shear characteristics of geosynthetic soil bags stacked in tilted and horizontal directions.,Geosynthetics Engineering Journal, JCIGS, Vol. 21, pp. 145-152. (in Japanese)
Mitsui-sanshi. 2018. Geo-tube DS. http://www.mitsui-sanshi.co.jp/syubetsu/s21-1.html, viewed on August 12, 2018. (in Japanese)
Miyata, Y. 2012. Reinforced soil walls during recent great earthquakes in Japan and geo-risk-based design. Earthquake Geotechnical Engineering Design. Geotechnical, Geological and Earthquake Engineering (Maugeri M. & Soccodato C., Eds.), Springer, Vol. 28, pp. 343-362. DOI= https://doi.org/10.1007/978-3-319-03182-8_12
Mohri, Y., Matsushima, K., Yamazaki, S., Lohani, T.N., Goran, A. & Aqil, U. 2007. New direction of earth reindorcement - disaster prevention. Proc. 5th Int. Symposium on Earth Reinforcement (IS-Kyushu 2007) -New Horizons in Earth Reinforcement- (Otani, J., Miyata, Y. and Mukunoki, T. Eds., Taylor & Francis), Fukuoka, Japan, pp. 85-101.
Mohri, Y., Matshushima, K., Hori, T., & Tani, S. 2005. Damage to small-size reservoirs and their reconstruction method, Special Issue on Lessons from the 2004. Niigataken Chu-Etsu Earthquake and Reconstruction, Foundation Engineering and Equipment (Kiso-ko), October, pp. 62-65. (in Japanese).
Murakami, K., Sato, S., et al. 2015. Effects of the erosion control performance of sand-packed containers in the Miyazaki coast. Journal of Coastal Engineering, JSCE, Vol. 71, No. 2, pp. 1135-1140. (in Japanese)
Tatsuoka, F., Tateyama, M., Mohri, Y. & Matsushima, K. 2007. Remedial treatment of soil structures using geosynthetic-reinforcing technology. Geotextiles and Geomembranes, Vol. 25 (4 & 5), pp. 204-220.
Tatsuoka, F., Tateyama, M., Koseki, J. & Yonezawa, T. 2013. Recent geosynthetic-reinforced soil structures for railways in Japan. Proc. 15th Conference on Current Researches in Geotechnical Engineering in Taiwan, Yunlin, Taiwan.
Tsunami Joint Survey Group 2012. Tohoku Earthquake Tsunami Information, http://www. coastal.jp/ttjt/, viewed on September 11, 2012.
US Geological Survey 2012. Magnitude 8 and Greater Earthquakes Since 1900, http:// earthquake.usgs. gov/earthquakes/eqarchives/year/mag8/magnitude8_1900_mag.php, viewed on September 11, 2012.
Watanabe, K., Nakajima, S., Fujii, K., Matsuura, K., Kudo, A. & Nonaka, T. 2017. Development of railway embankment resistant to sever earthquakes and prolonged overflows caused by Tsunami. Proc. 19th International Conference on Soil Mechanics and Geotechnical Engineering, Seoul, Korea, pp.2937-2940.